Binding of a Macrocyclic Bisacridine and Ametantrone to CGTACG Involves Similar Unusual Intercalation Platforms†

Xiang-lei Yang,‡ Howard Robinson, Yi-Gui Gao, and Andrew H.-J. Wang*

Department of Biochemistry, School of Molecular & Cellular Biology, University of Illinois at Urbana-Champaign, Urbana, Illinois 61801

Received June 8, 2000; Revised Manuscript Received July 17, 2000

ABSTRACT: The binding of a macrocyclic bisacridine and an antitumor intercalator ametantrone to DNA has been studied. We carried out X-ray diffraction analyses of the complexes between both intercalators and CGTACG. We have determined the crystal structure, by the multiple-wavelength anomalous diffraction (MAD) method, of bisacridine complexed with CGTA[br^{5}C]G at 1.8 Å resolution. The refined native crystal structure at 1.1 Å resolution (space group *C*222, $a = 29.58$ Å, $b = 54.04$ Å, $c = 40.22$ Å, and *R*-factor = 0.163) revealed that only one acridine of the bisacridine drug binds at the C5pG6 step of the DNA, with the other acridine plus both linkers completely disordered. Surprisingly, both terminal G·C base pairs are unraveled. The C1 nucleotide is disordered, and the G2 base is bridged to its own phosphate P2 through a hydrated Co^{2+} ion. G12 is swung toward the minor groove with its base stacked over the backbone. The C7 nucleotide is flipped away from the duplex part and base paired to a 2-fold symmetry-related G6*. The central four base pairs adopt the B-DNA conformation. An unusual intercalator platform is formed by bringing four complexes together (involving the 222 symmetry) such that the intercalator cavity is flanked by two sets of G·C base pairs (i.e., C5·G8 and G6·C7*) on each side, joined together by G6·G8* tertiary base pairing interactions. In the bisacridine−CGTACG complex, the intercalation platform is intercalated with two acridines, whereas in the ametantrone−CGTACG complex, only one ametantrone is bound. NMR titration of the bisacridine to AACGATCGTT suggests that the bisacridine prefers to bridge more than one DNA duplex by intercalating each acridine to different duplexes. The results may be relevant in understanding binding of certain intercalators to DNA structure associated with the quadruplet helix and Holliday junction.

Intercalators, by definition, bind to DNA by intercalating the flat aromatic ring between base pairs of DNA duplex. While the manner in which intercalators insert themselves into the intercalation cavity may be different, the distortion of the duplex is more or less similar, involving the stretching of adjacent base pair separation to 6.8 Å (from 3.4 Å) and various extents of helix unwinding (*1*). In almost all the structures of intercalator−DNA complexes that have been determined thus far (*2*), the base pairs surrounding the intercalator cavity remain essentially intact, except in one case. This observation is also valid for bis-intercalators. The only exception known so far is found in the structure of a DNA−porphyrin complex (*3*). In that structure, the extremely bulky size of the copper(II) *meso*-tetrakis(*N*-methylpyridyl)-porphyrin ring could not be accommodated in a canonical intercalation cavity and caused a nucleotide next to the porphyrin ring to flip out.

A macrocyclic 9-aminoacridine-containing bis-intercalator (abbreviated as bisacridine; Figure 1A) has been synthesized with the aim that it can bind DNA by threading the two linkers across base pairs so that the linkers reside in both minor and major grooves simultaneously. Its binding to DNA has been studied (*4*). However, the addition of bisacridine to DNA solutions often resulted in serious precipitation, making biophysical analysis difficult. On the basis of the interactions of bisacridine with CGCG, different threading models have been proposed (*4*). But whether bisacridine actually threads DNA or what the binding size and sequence are remains unclear.

Another intercalator that may have the potential of binding DNA by a threading mechanism is the clinically useful anticancer drug mitoxantrone (and its analogue ametantrone) (Figure 1A). These two drugs have two long chains symmetrically located on opposite sides of the anthraquinone ring. It remains to be elucidated how the three-ring anthraquinone inserts itself between base pairs. Does it intercalate with its long axis parallel with [like in acridine orange (*5*), or 9-aminoacridine derivative DACA (*6*)] or perpendicular to [like in anthracycline drugs daunorubicin and nogalamycin (*1*, *2*)] the C1′−C1′ lines? In the former parallel mode, the two long side chains would be forced to thread through the base pairs and to be located in the opposite grooves. Conversely, in the latter perpendicular bayonet mode, both side chains would reside in the same groove.

Here, we study by X-ray crystallography the structures of bisacridine and ametantrone complexed to CGTACG at high

† This work was supported by the American Cancer Society (Grant RPG-94-014-06) and the NSF (Grant MCB98-08298) to A.H.-J.W.

* To whom correspondence should be addressed. Telephone: (217) 244-6637. Fax: (217) 244-3181. E-mail: ahjwang@uiuc.edu.

‡ Present address: Department of Molecular Biology, The Scripps Research Institute, La Jolla, CA.

10.1021/bi001319z CCC: $19.00
Published on Web 08/17/2000

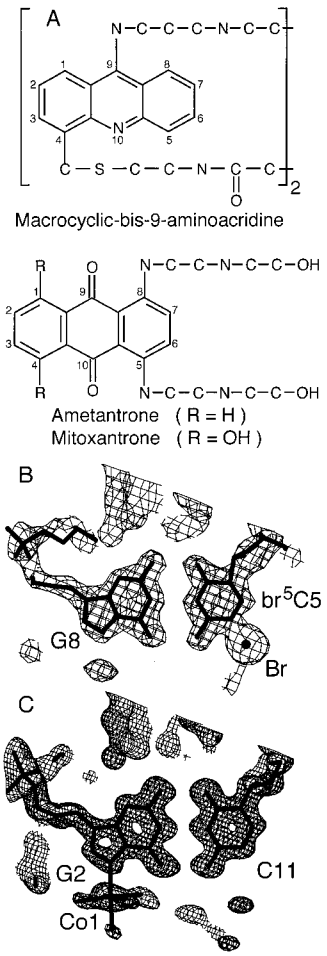

FIGURE 1: (A) Molecular formula of the macrocyclic bisacridine and mitoxantrone and/or ametantrone. Most hydrogen atoms are not shown. (B) Fourier electron density map (contoured at the 1.8σ level) of the G8·br^{5}C5 base pair of the bisacridine−CGTA[br^{5}C]G complex after density modification of the MAD phases at 1.8 Å resolution was applied. (C) Refined ($2F_o - F_c$) Fourier electron density map (contoured at the 1.8σ level) of the G2·C11 base pair of the bisacridine−CGTACG complex at 1.1 Å resolution.

resolution and compare them to those of related intercalator−DNA complexes (*1*, *2*) to improve the understanding of the binding properties of those intercalators. Surprisingly, we discovered that both drugs do intercalate DNA, but create a highly unusual intercalation platform in which the drugs are flanked by a quadruplet of bases (generated from two sets of G·C base pairs).

MATERIALS AND METHODS

The DNA molecules, including the brominated derivatives, were synthesized at the DNA synthesis facility at University of Illinois at Champaign-Urbana and purified by gel-filtration column chromatography. Crystals were obtained from solutions having 1.3 mM DNA single strand, 1.3 mM drug (bisacridine or ametantrone), 40 mM sodium cacodylate buffer (pH 6.0), 10 mM $MgCl_2$, 1 mM $CoCl_2$, 3 mM spermine, and 4% 2-methyl-2,4-pentanediol (2-MPD)[1], equilibrated with 30 mL of 50% 2-MPD, using the vapor diffusion method (*7*). Their crystallographic statistics are listed in Table 1. Diffraction data were measured at 110 K at Structural Biology Center undulator beamline 19ID at the Advanced Photon Source using fundamental undulator harmonics and 3×3 mosaic CCD detector as described previously (*8*, *9*). Crystallographic data integration and reduction were carried out with the program package HKL2000 (*10*).

Experimental phases from the CGTA[br^{5}C]G−bisacridine complex crystal were obtained by the MAD method using the approach similar to that described recently (*8*, *9*). Two bromine sites were found using the Patterson heavy atom search method, and the phases were calculated semiautomatically as implemented in the crystallographic suite CNS (*11*). The figure of merit is 0.83 and 0.96 before and after density modification, respectively. The resulting electron density map at 1.8 Å resolution were of high quality, revealing not only the DNA chain but also the metal ions and many water molecules bound to DNA (Figure 1B). Some of the essential statistics of the MAD phasing are given in Table 1. The structure of the ametantrone−CGTACG complex was subsequently determined by the molecular replacement method.

Both structures have been refined, first by the simulated annealing procedure incorporated in X-PLOR (*12*) and then by SHELX97 (*13*). The DNA force field parameters of Parkinson et al. (*14*) with modifications to allow sugar pucker to vary were used. Water molecules were located by the procedure incorporated in SHELX97. We were careful in the criteria of the inclusion of water molecules. Only first-shell waters and well-defined higher-shell waters were included. For the bisacridine−DNA complex, anisotropic temperature factors were applied for all atoms of DNA and two hydrated Co^{2+} ions, and isotropic temperature factors were applied for nonliganded water molecules. No hydrogen atoms were included. For the ametantrone−DNA structure, all atoms were treated with isotropic temperature factors. For both structures, the procedure of SWAT in SHELX97 by Moews and Kretsinger (*15*) has been applied to model the diffuse solvent. The atomic coordinates of the two crystal structures have been deposited at the Research Collaboratory for Structural Bioinformatics (RCSB) Protein Data Bank (accession number 1FD5 for the bisacridine structure and 1FDG for the ametantrone structure). The procedure for the NMR titration of the drug and DNA follows that described by Yang et al. (*16*).

RESULTS AND DISCUSSION

Molecular Structure of the Bisacridine−CGTACG Complex. The bisacridine−CGTACG complex has been crystallized in the presence of Mg^{2+} and Co^{2+} ions. The structure was determined by the MAD method using the CGTA[br^{5}C]G crystal. The native structure was then refined to 1.1 Å resolution to an *R*-factor of 16.3%. The ametantrone−CGTACG complex was subsequently determined by molecular replacement (MR). Since the bisacridine structure has very good quality, most of the discussion is based on this structure.

The refined structure of the bisacridine−CGTACG complex, shown in Figure 2A, contains many unexpected features. There is one bisacridine bound to one partially

[1] Abbreviations: NMR, nuclear magnetic resonance; rmsd, root-mean-square deviation; SA, simulated annealing; MPD, 2-methyl-2,4-pentanediol; PEG400, polyethylene glycol 400; br^{5}C, 5-bromodeoxycytidine.

Table 1: Crystallographic and Refinement Data of CGTACG−Bisacridine and CGTACG−Ametantrone Complexes

	bisacridine complex				ametantrone complex
	0.7251 Å high-resolution	0.9199 Å[a] peak	0.9200 Å[a] inflection point	0.8856 Å[a] high-remote	0.7251 Å
crystallographic data					
a (Å)	29.58	29.14	29.14	29.14	29.09
b (Å)	54.04	54.90	54.89	54.90	52.71
c (Å)	40.22	39.88	39.88	39.88	40.18
space group	*C*222	*C*222	*C*222	*C*222	*C*222
resolution (Å)	1.1	1.8	1.8	1.8	1.6
no. of observed reflections	196823	80537	80633	80757	57036
$\langle I/\sigma(I)\rangle$	40.54	31.97	35.81	47.77	32.48
phasing power		3.5	6.2	3.8	
no. of unique reflections	13377	5694	5693	5668	4270
R_{merge} (%)	5.7	5.0	4.5	3.7	5.2
completeness (%)	99.9	99.8	99.8	99.5	99.1
refinement data					
no. of reflections [$>2.0\ \sigma(I)$]	10367				3106
R-factor/*R*-free (5% data)	0.163/0.203				0.249/0.314
rmsd for bond distances (Å)	0.014				0.008
rmsd for bond angles (deg)	2.0				1.7
no. of DNA atoms	225				225
no. of waters	68				20
no. of cations	1.5 Co				1.5 Co
	0.5 Mg				0.5 Mg

[a] DNA is CGTA[br^{5}C]G.

unraveled $(CGTACG)_2$ duplex in the asymmetric unit. However, only one acridine ring is found to intercalate between the C5pG6 step. No electron density could be seen for the other acridine ring and most of the linker atoms, which are presumably disordered. The intercalated acridine has its 9-amino group pointing toward the major groove direction. The electron density associated with the intercalated acridine (Figure 1S) suggests that the acridine may adopt two positions by rotating 180° about the C9·N10 line.

Both terminal G·C base pairs (C1·G12 and G6·C7) are completely unraveled, leaving only the central four base pairs in the duplex form. The central tetranucleotide duplex backbone torsion angles adopt B-DNA-like values with a few exceptions (Table 1S). The average values (excluding outliers) are as follows: α, 295.5°; β, 177.2°; γ, 50.5°; δ, 135.8°; ϵ, 186.6°; ζ, 270.6°; and χ, 252.3°. The most apparent deviations are associated with the looped-out nucleotides C7 ($\zeta = 68.6°$) and G8 ($\alpha = 54.9°$), i.e., a *gauche*$^+$/*gauche*$^+$ conformation for the C7pG8 step. Most of the sugars have the S-type pucker (*C2′-endo*) with an averaged pseudorotation angle of 132.7°, except for 3′-terminal G6, G12, and G8 which are of the N-type pucker. The extension of the C5pG6 step for the intercalation of acridine is achieved by a combination of a large β value and the *C3′-endo* pucker of the G6 sugar.

The Terminal Nucleotides Are Looped Out, Providing Tertiary Base Interactions. Both terminal G·C base pairs adopt a looped-out conformation. Interestingly, despite the high-resolution nature of the crystal, the C1 nucleoside is completely disordered. The phosphate of G2 is ordered, leaving an intact 5′-PO_4^-. A pentahydrated Co^{2+} ion is coordinated to G2N7 with the hydration sphere hydrogen bonded to the G2 phosphate and bases. We were curious to know whether the C1(O3′−P) bond is hydrolyzed in the crystallization dips in the presence of intercalator, Co^{2+}, or Mg^{2+}. We collected crystals of the bisacridine−CGTACG complex, washed them extensively with and dissolved them in distilled water, and subjected the dissolved solution to electrospray ion (ESI) mass spectrometry. The resulting ESI mass spectra showed only the presence of intact CGTACG (mass of 1792.3). No 5′-pGTACG peak (mass of 1582.3) could be detected. The results support the argument that the C1 nucleoside is crystallographically disordered, rather than hydrolyzed. The G12 nucleotide is twisted away such that the guanine base is folded back and stacked over the backbone of the C11·G12 nucleotides.

At the other end of the duplex, one acridine is intercalated between the C5pG6 step (Figure 2A). The 5′-terminal C7 nucleotide is flipped away, involving mostly the δ of C7 and α of G8 torsion angles, and a change of the G8 sugar pucker to the N type.

A Novel Intercalation Platform. The extended C7 is actually Watson−Crick base paired with G6* from a 2-fold symmetry-related complex. This can be more clearly seen in Figure 2B. Two complexes (pink and cyan) related by the 2-fold operation are stacked end over end to create a part of a large "intercalation platform" in which two acridine rings (purple) are intercalated.

The G8 from the pink complex is base paired with the G6 of the green complex from the minor groove side through the G8N2−G6N3 (2.99 Å) and G8N3−G6N2 (3.07 Å) hydrogen bonds. [This type of G·G base pairing is commonly seen in DNA crystal structures (*17*).] In addition, the G6 from one complex is base paired with the extruded C7 nucleotide (orange at left and light-green color at right) of other 2-fold related complexes. Therefore, each side of the intercalation platform has two G·C base pairs (C5·G8 and G6·C7#) linked together through the G6·G8* tertiary base pair (where # and ∗ represent different symmetry-related 2-fold operations). A closeup view of the intercalation platform is shown in Figure 3.

The complete intercalation is generated involving four crystallographically related complexes using 222 symmetry. Figure 2S shows the crystal packing interactions of two

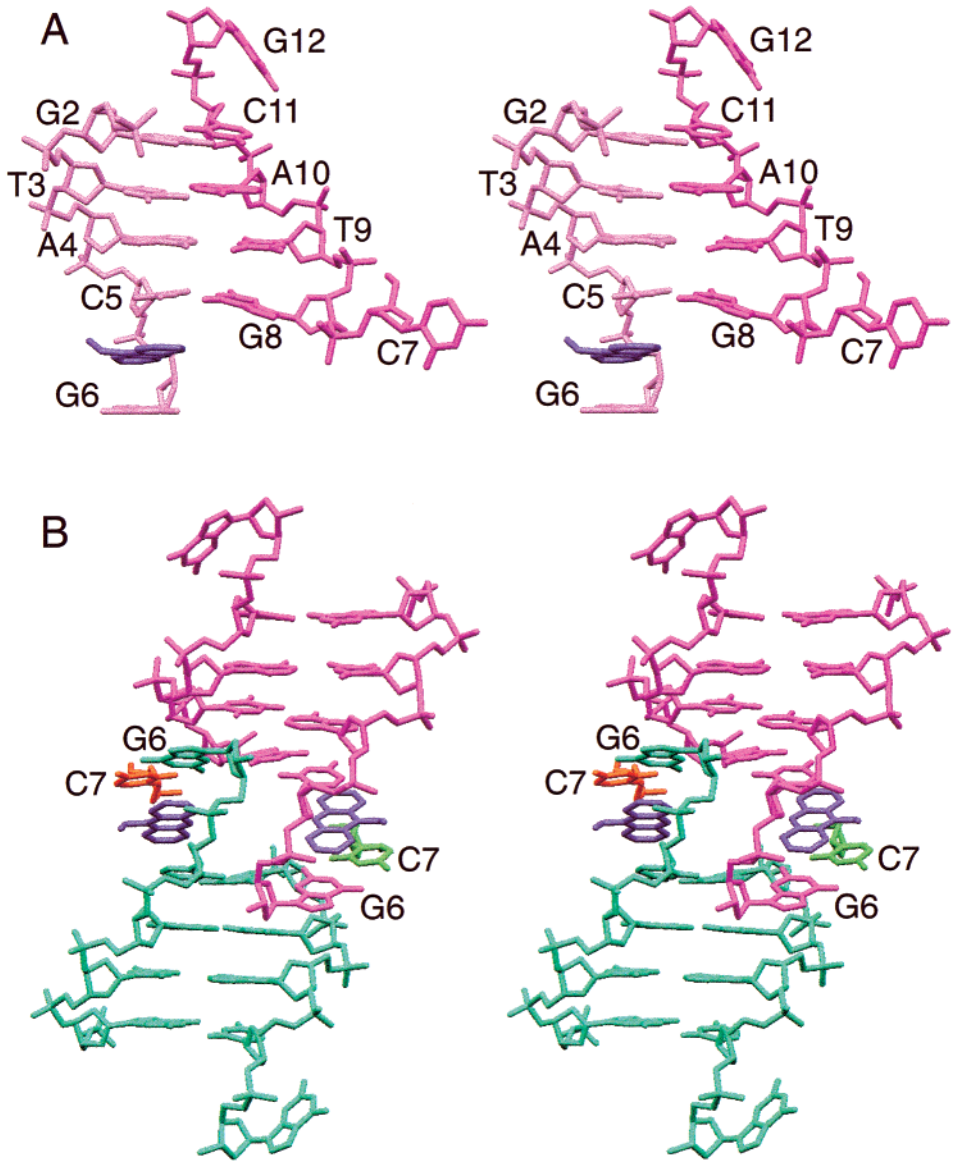

FIGURE 2: (A) Structure of the bisacridine−CGTACG complex. Both terminal G·C base pairs are unraveled with the C1 nucleoside completely disordered. The G12 nucleotide is twisted away such that the guanine base is stacked over the backbone of C11. One acridine is intercalated between the C5pG6 step. (B). Two complexes (pink and cyan) related by the 2-fold operation are stacked end over end to form part of a large intercalation platform in which two acridine rings (purple) are intercalated. The G8 from the pink complex is base paired with G6 of the cyan complex from the minor groove side through the G8N2−G6N3 and G8N3−G6N2 hydrogen bonds. In addition, the G6 from one complex is base paired (in a Watson−Crick conformation) with the flipped out C7 nucleotide (orange and green) of other 2-fold related complexes. Therefore, each side of the intercalation platform has two G·C base pairs (C5·G8 and G6-C7$^{\#}$) linked together through a G6·G8* tertiary base pair (where $^{\#}$ and * represent different symmetry-related 2-fold operations).

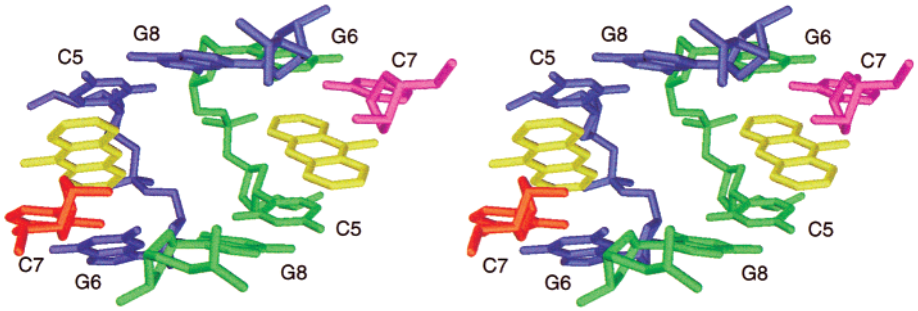

FIGURE 3: Closeup side view of the intercalation platform. For clarity, the coloring scheme is different from that in Figure 2. The blue molecule is from the reference molecule at (x, y, z). The green, orange, and purple molecules are from the 2-fold symmetry-related complexes at ($1-x$, $-y$, z), ($1-x$, y, $1-z$), and (x, $-y$, $1-z$), respectively. The acridines are gold. This view is along the 2-fold axis in the c-axis direction.

dimeric complexes (see Figure 2B). The adjacent columns of the duplexes have a left-handed crossover angle of ~53°.

The detailed conformation of the intercalation platform involves two sets of quadruplet base pairs in the bisacridine−

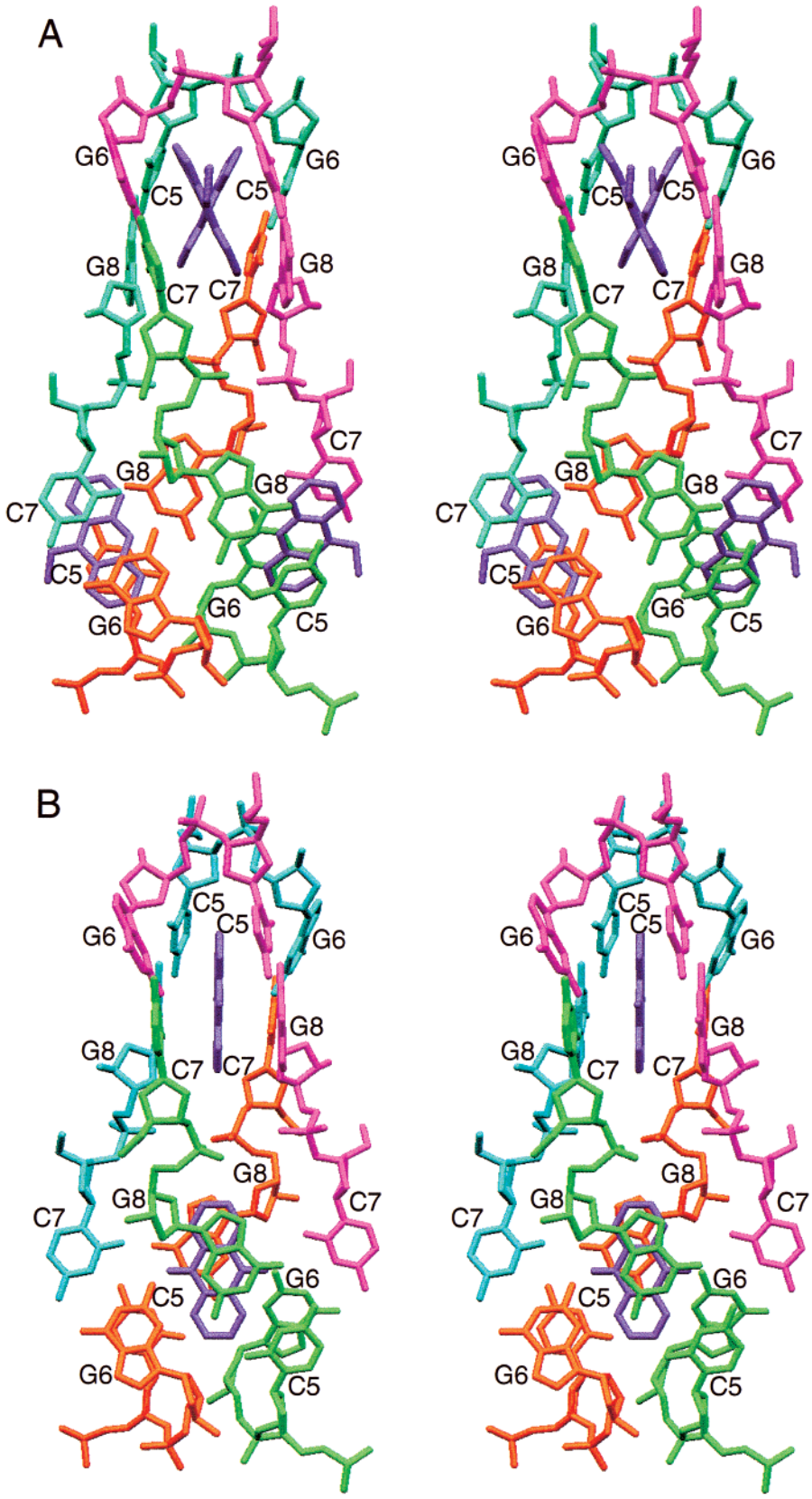

FIGURE 4: (A) Detailed conformation of the intercalation platform involving two sets of quadruplet base pairs in the bisacridine−CGTACG complex. Here four complexes, related by 222 symmetry, are bound together by base pairing interactions. In this view, a vertical 2-fold axis is evident. There is a significant dihedral angle (34°) between the C5·G8 and G6·C7 base pairs, and a large dihedral angle (54°) between two symmetry-related acridines, which are about 11 Å apart. No electron density could be seen in the region between the two acridines. (B) Corresponding intercalation platform in the ametantrone−CGTACG complex.

CGTACG complex (Figures 3 and 4A). Here four complexes, related by 222 symmetry, are bound together by base pairing interactions. In this view, a vertical 2-fold axis is evident. In the top part of Figure 4A, it can be seen that there is a

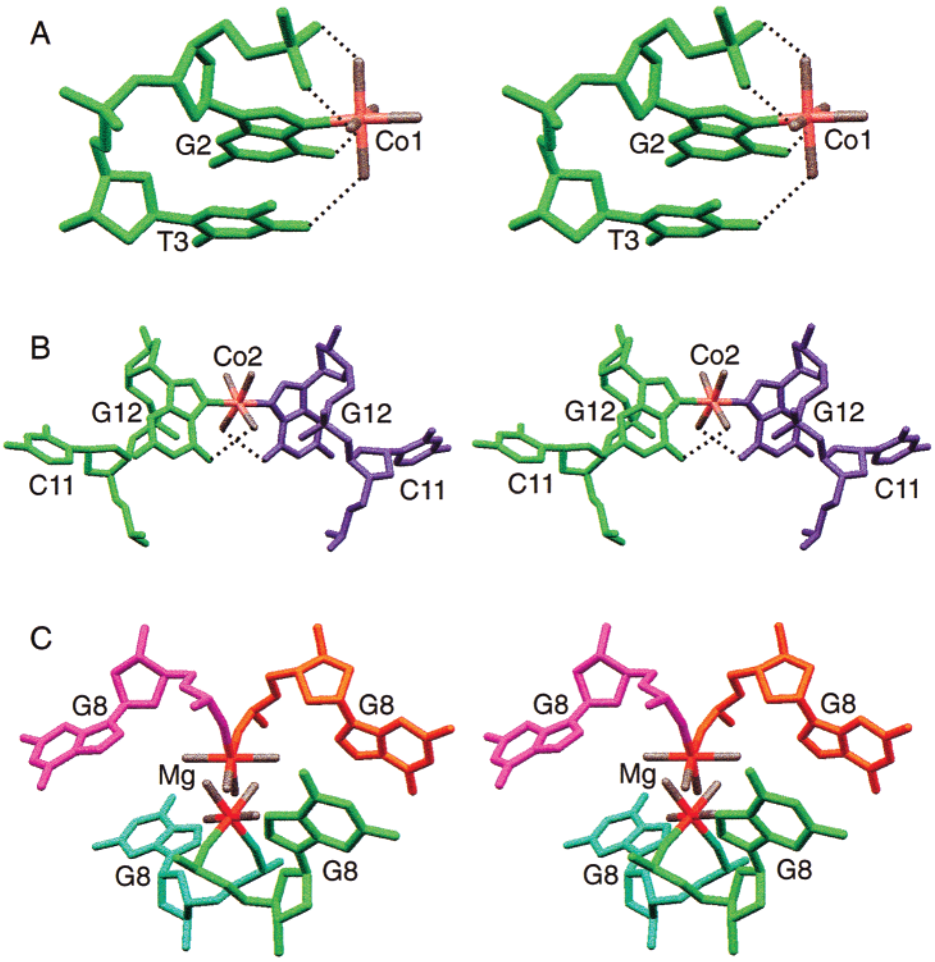

FIGURE 5: Interactions of metal ions with DNA. Nucleotides from different symmetry-related duplexes are colored differently. (A) The pentahydrated Co^{2+} ion coordinated at the G2N7. The hydration sphere of Co^{2+} ion is extensively hydrogen bonded to DNA, including the phosphate of the G2 nucleotide. The C1 nucleotide is disordered. (B) A quadrahydrated Co^{2+} ion bridging two symmetry-related G12N7 sites. (C) A disordered quadrahydrated Mg^{2+} ion interacts with four symmetry-related G8 nucleotides. The Mg^{2+} ion is directly coordinated to the oxygens of P8 phosphates.

significant dihedral angle (34°) between the C5·G8 and G6·C7 base pairs, and a large dihedral angle (54°) between two symmetry-related acridines, which are about 11 Å apart. In the lower part of Figure 4A, the acridine rings are clearly seen to locate near the two edges of the platform. The acridine ring has the G6·C7 base pair stacked on one side and the C5 base stacked on the other side. The long axis of the acridine ring is nearly parallel to the C1′−C1′ line of the G6·C7 base pair, and its 9-amino group points in the major groove direction and away from the center of the platform. Since the 9-amino groups of the two symmetry-related acridines point in the opposite direction, it is unlikely that the spermine linker can span through the inside of the intercalation platform.

This is also supported by the fact that no electron density could be seen in the region between the two acridines. Therefore, it seems more plausible that the peptide linker winds out from inside of the platform and joins the other acridine of the bisacridine in the solvent region. There is sufficient room in the solvent region to accommodate the dangling part of the bisacrdine as shown in panel A of Figure 2S. Because of the flexibility of both spermine and peptide linkers, the outside acridine and the linkers are disordered. The possibility of the linkers becoming broken was considered, but deemed unlikely. The mass spectra derived from the dissolved crystals did not have obvious peaks that could be associated with the monomer of bisacridine. The NMR titration also supported a fully linked, sysmetrical, bisacridine.

Although the intercalation platform in the ametantrone−CGTACG complex is similar to that of the bisacridine−CGTACG complex, some differences are seen. The location of ametantrone is shifted to the center of the intercalation platform, coinciding with a 2-fold axis (Figure 4B). The drug is stacked between two symmetry-related G8 bases. This is consistent with the observation that the vertical distance between the two G8 planes is reduced from ~8.0 Å in the bisacridine−CGTACG complex to ~6.8 Å in the ametantrone−CGTACG complex.

Interactions of Metal Ions with the Drug−DNA Complexes. The availability of the atomic resolution structure provides an excellent opportunity to inspect the interactions of water molecules and ions with DNA, and interactions between DNA. Three metal ions were located (Figure 5), and they play important roles in the crystal lattice interactions. A pentahydrated Co^{2+} ion coordinated to the G2·N7 site was found in a nested cavity in the major groove near the G2pT3 step. The Co^{2+} ion-bound water molecules are hydrogen bonded to the neighboring P2 phosphate oxygens (Figure 5A). A second Co^{2+} ion is used to bridge

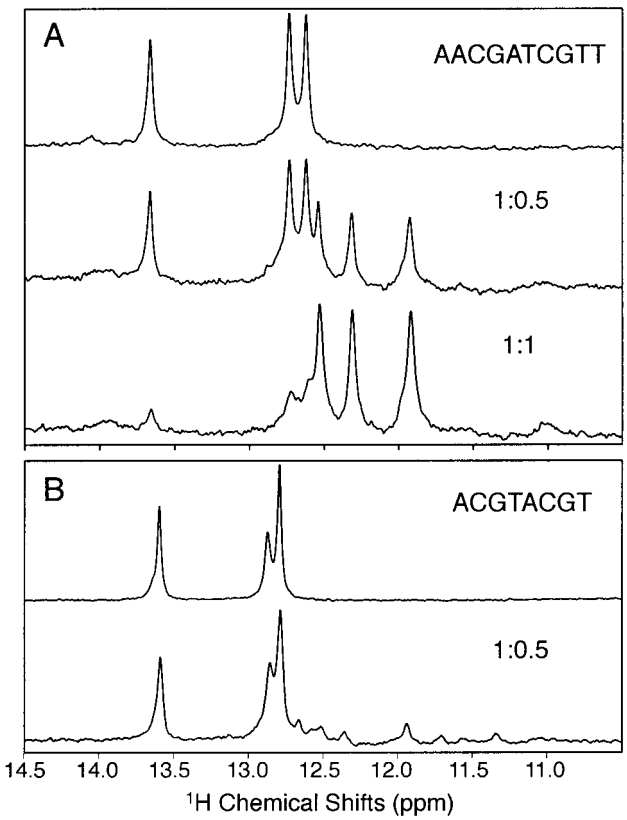

FIGURE 6: Titration of bisacridine with (A) AACGATCGTT and (B) ACGTACGT, monitored by the imino proton resonances of the proton one-dimensional NMR spectra (2 °C) at 500 MHz. In panel A, at a drug:DNA ratio of 0.5:1, proton resonances from both free DNA and bound DNA are present simultaneously, indicating the slow exchange rate between the free and bound drug. In panel B, only small amounts of the imino proton resonances from the bound complex were seen. When the drug:DNA ratio reached 1:1, most of the drug−DNA complex precipitated.

two symmetry-related G12 bases by coordinating to their N7 sites (Figure 5B). This Co^{2+} ion (labeled Co2) is responsible for the lattice interactions on the G12 end of the complex.

Finally, a cavity surrounded by four phosphates from symmetry-related G8 nucleotides is filled with a 2-fold disordered $Mg(H_2O)_4^{2+}$ ion, neutralizing the cluster of negative phosphate charges.

Binding of Bisacrdine to DNA in Solution Studied by NMR. The design of the macrocyclic bisacridine was intended for binding DNA double helix through the bis-intercalating mode with the two linkers threading both the major and minor grooves simultaneously. Since the fully extended distance of both linkers is about 16 Å, comparable to the stacking distance spanning four base bases, it is possible that a DNA sequence such as CGNNCG should be a suitable DNA binding sequence for bisacridine. We chose AACGATCGTT and ACGTACGT for our NMR structural study.

Addition of bisacridine to solutions of AACGATCGTT caused large upfield shifts in the NMR spectra of the imino proton resonances (Figure 6A). At a 0.5:1 (drug:DNA duplex) ratio, new resonances emerged, and they existed simultaneously with the free DNA resonances, suggesting that the binding equilibrium between the free DNA and drug−DNA complex is in the slow exchange regime. In going from a 0.5:1 ratio to a 1:1 ratio, the spectrum simplified so that there is only one resonance per proton, indicating that the 1:1 complex is 2-fold symmetrical. In contrast, at a 0.5:1 bisacridine:$(ACGTACGT)_2$ ratio, only small peaks of new imino proton resonances appeared (Figure 6B). This was due to the fact that most of the complex precipitated. In addition, the number of new resonances appears to be more than three, indicating that the complex is not 2-fold symmetrical or multiple species of complexes exist. In both titrations, severe precipitation occurred which resulted in very low concentrations of the complexes in solution and made two-dimensional NMR experiments impractical. Heating and slow cooling to reanneal the drug−DNA complex in the sample solutions did not improve the solubility of the complex.

We interpret those results as follows. First, the CpG step as the most preferred intercalation site is well-established. Thus, it is expected that the acridine moiety of bisacridine would intercalate at the CpG sites in AACGATCGTT. The two CpG sites are separated by 17 Å (3.4 × 5 Å), too far to be reached energetically favorably by the fully extended linkers, contrary to what we predicted. It is more likely that one bisacridine binds to two different duplexes by intercalating each acridine to a CpG site from different duplexes. Such a binding mechanism would result in cross-linking and aggregation of complexes, consistent with the observation that precipitation occurred readily during titration of bisacridine to DNA. The precipitation may be aided by the charge neutralization between bisacridine (+5 charges) and DNA.

The molecular species that remains soluble in solution (at low concentrations) is likely the 2:2 bisacridine−$(AACGATCGTT)_2$ dimeric form, which is 2-fold symmetric, consistent with the tiration spectra (Figure 6A). In the titration of bisacridine to ACGTACGT, nearly all complexes are precipitated (leaving very little complex in solution), likely due to a more complete charge neutralization. Furthermore, the TpA site provides another favorable intercalation site. The multiple intercalation sites of ACGTACGT would produce a complex mixture of oligomeric drug−DNA complexes, consistent with the large number of new upfield-shifted imino proton resonances (Figure 6B).

It should be emphasized that, due to the disposition of the two linkers on the acridine ring, the intercalation of the acridine ring with its linkers would result in a collateral disruption of base pairing structure, as evident from the present crystal structures.

Comparison with Other Intercalation Motifs and Biological Implications. All structures of the intercalator−DNA complexes that have been analyzed so far have a similar canonical intercalation pattern, i.e., a stretching of adjacent base pairs to 6.8 Å to accommodate the aromatic intercalator ring (*1*, *2*). Although alternative base pair schemes, e.g., Hoogsteen (*18*) or reverse Watson−Crick (*19*), have been observed, no disruption of base pair has been seen so far, except in one case. In the two structures presented here, a major disruption of base pair adjacent to the intercalator occurred, which resulted in a novel, heretofore unseen, intercalation platform.

The binding of bisacridine in the intercalation platform is reminiscent of the model of 9-aminoacridine bound to the cyclic (pGpG) dinucleotide structure (*20*). In that model, an intercalation platform is created by joining four cyclic

(pGpG) dinucleotides together, using a circular G-quartet hydrogen bonding scheme. In fact, some intercalators have been shown to have a binding preference for G-quartet structure (reviewed in ref *21*). For example, a porphyrin derivative has been shown to bind to the T_4G_4 quadruplet structure (*22*). As mentioned before, the crystal structure of a porphyrin−DNA complex revealed that porphyrin disrupts a canonical intercalation cavity (*3*) and is likely to prefer a large intercalation platform, similar to that found in the present structures, or a G-quartet structure. Our structures here lend support to the idea that nonconventional intercalation structures are possible.

It is of interest to note that the way in which the C7 nucleotide performs a strand switch to base pair with G6 (in Watson−Crick conformation) bears a strong resemblance to that found in the crystal structure of a DNA Holliday junction (*23*). It is possible that binding of certain intercalators to DNA may facilitate the strand exchange process. Conversely, the Holliday junction structure in the DNA recombination process may be a preferred target site for certain intercalators.

Mitoxantrone is a known poison of topoisomerase II (*24*). The disruption of a base pair at the drug intercalation site may be relevant in the ternary interactions among drug, DNA, and topoII. In the model of the ternary cleavable complex of camptothecin, DNA, and topoisomerase I, the base pair next to the intercalated camptothecin is unraveled (*25*), not unlike that seen in the structure presented here.

In conclusion, the findings that certain intercalators and bis-intercalators can induce a novel intercalation platform provide new insights into the design of future DNA intercalating drugs. Multistranded DNA structures may be considered as a new family of potential drug targets. Study along this direction is underway.

ACKNOWLEDGMENT

We thank Dr. S. Zimmerman for providing the macrocyclic bisacridine compound and Dr. K. Murdock of American Cyanamide Co. for the ametantrone. We thank W. Minor (University of Virginia, Charlottesville, VA) for making HKL2000 available to us before its official release. The technical help of Drs. A. Joachimiak and R. Sanishvili in the use of beamline ID19 is gratefully acknowledged.

SUPPORTING INFORMATION AVAILABLE

One table of the torsion angles and helical parameters of the two crystal structures and two figures of electron density of acridine and ametantrone, with crystal packing diagrams of the DNA included. This material is available free of charge via Internet at http://pubs.acs.org.

REFERENCES

1. Wang, A. H.-J. (1992) *Curr. Opin. Struct. Biol. 2*, 361−368.
2. Yang, X.-L., and Wang, A. H.-J. (1999) *Pharmacol. Ther. 83*, 181−215.
3. Lipscomb, L. A., Zhou, F. X., Presnell, S. R., Woo, R. J., Peek, M. E., Plaskon, R. R., and Williams, L. D. (1996) *Biochemistry 35*, 2818−2823.
4. Veal, J. M., Li, Y., Zimmerman, S. C., Lamberson, C. R., Cory, M., Zon, G., and Wilson, W. D. (1990) *Biochemistry 29*, 10918−10927.
5. Wang, A. H.-J., Quigley, G. J., and Rich, A. (1979) *Nucleic Acids Res. 12*, 3879−3890.
6. Adams, A., Guss, J. M., Collyer, C. A., Denny, W. A., and Wakelin, L. P. G. (1999) *Biochemistry 38*, 9221−9233.
7. Wang, A. H.-J., and Gao, Y.-G. (1990) *Methods 1*, 91−99.
8. Walsh, M. A., Evans, G., Sanishvili, R., Dementieva, I., and Joachimiak, A. (1999) *Acta Crystallogr. D55*, 1726−1732.
9. Gao, Y.-G., Robinson, H., Sanishvili, R., Joachimiak, A., and Wang, A. H.-J. (1999) *Biochemistry 38*, 16452−16460.
10. Otwinowski, Z., and Minor, W. (1997) *Methods Enzymol. 276*, 307−326.
11. Brünger, A. T., Adams, P. D., Clore, G. M., DeLano, W. L., Gros, P., Grosse-Kunstleve, R. W., Jiang, J. S., Kuszewski, J., Nilges, M., Pannu, N. S., Read, R. J., Rice, L. M., Simonson, T., and Warren, G. L. (1998) *Acta Crystallogr. D54*, 905−921.
12. Brünger, A. T. (1992) *X-PLOR 3.1, A System for X-ray Crystallography and NMR*, Yale University Press, New Haven, CT.
13. Sheldrick, G. M. (1997) *SHELX-97, crystallographic refinement program*, University of Gottingen, Gottingen, Germany.
14. Parkinson, G., Vojtechovsky, J., Clowney, L., Brunger, A. T., and Berman, H. M. (1996) *Acta Crystallogr. 52*, 57−64.
15. Moews, P. C., and Kretsinger, R. H. (1975) *J. Mol. Biol. 91*, 201−228.
16. Yang, X.-L., Kaenzig, C., Lee, M., Sugiyama, H., and Wang, A. H.-J. (1999) *Nucleic Acids Res. 27*, 4183−4190.
17. Coll, M., Sherman, S. E., Gibson, D., Lippard, S. J., and Wang, A. H.-J. (1990) *J. Biomol. Struct. Dyn. 8*, 315−330.
18. Wang, A. H.-J., Ughetto, G., Quigley, G. J., Hakoshima, T., van der Marel, G. A., van Boom, J. H., and Rich, A. (1984) *Science 225*, 1115−1121.
19. Dutta, R., Gao, Y.-G., Priebe, W., and Wang, A. H.-J. (1998) *Nucleic Acids Res. 26*, 2981−2988.
20. Guan, Y., Gao, Y.-G., Liaw, Y.-C., Robinson, H., and Wang, A. H.-J. (1993) *J. Biomol. Struct. Dyn. 11*, 253−276.
21. Han, H., and Hurley, L. H. (2000) *Trends Pharmacol. Sci. 21*, 136−142.
22. Anantha, N. V., Azam, M., and Sheardy, R. D. (1998) *Biochemistry 37*, 2709−2714.
23. Ortiz-Lombardia, M., Gonzalez, A., Eritja, R., Aymami, J., Azorin, F., and Coll, M. (1999) *Nat. Struct. Biol. 6*, 913−917.
24. Hande, K. R. (1998) *Biochim. Biophys. Acta 1400*, 173−184.
25. Redinbo, M. R., Stewart, L., Kuhn, P., Champoux, J. J., and Hol, W. G. (1998) *Science 279*, 1504−1513.

BI001319Z